STEADY 2D CONDUCTION IN HETEROGENEOUS MEDIA WITH SIMPLE BOUNDARY CONDITIONS: COMBINED GITT-FVM SOLUTION

Thayná da Fonseca Rangel, thaynaarangel@gmail.com[1]
Leandro Alcoforado Sphaier, lasphaier@id.uff.br[1]
[1]Laboratory of Thermal Sciences. Department of Mechanical Engineering, Universidade Federal Fluminense – PGMEC/UFF. Rua Passo da Pátria 156, bloco E, sala 206-D, Niterói, RJ, 24210-240, Brazil.

Abstract: *The purpose of this work is to develop a combined integral-transform finite-volumes solution to heat conduction problems in heterogeneous materials. The considered problem comprises steady two-dimensional heat conduction in a heterogeneous medium composed of a polymeric matrix with low thermal conductivity and a metallic filler with higher thermal conductivity. Dirichlet boundary conditions are applied at the top and bottom surfaces, while the remaining boundaries are kept insulated. The Generalized Integral Transform Technique combined with a second-order Finite Volumes scheme were used to develop a hybrid numerical-analytical solution to the problem, which was implemented in the Mathematica system. Convergence results of temperature at selected positions are then analysed, showing that with 40 terms in the series and 50 divisions in the FVM grid, an error of about 1% is assured.*
Keywords:*heat conduction, conductivity, polymers*

1. INTRODUCTION

Polymers has found many applications in electronics industry due its corrosion resistance, low density and easy processing (Shi *et al.*, 2009; Zhao *et al.*, 2013; Agrawal and Satapathy, 2015). For these applications, it's important that the material has a high thermal conductivity, due the necessity of faster devices that dissipate bigs amounts of energy, but polymers has thermal conductivity around 0.1 $\mathrm{W.m^{-1}.K^{-1}}$, which is not enough for this case (Zhao *et al.*, 2013; Lee *et al.*, 2006) .

Researchers have been studying ways of enhancing the thermal conductivity of polymers using different processes, some of them using metal fillers with different shapes and sizes. Moreira *et al.* (2015) estimated the increase in thermal conductivity of a composite of epoxi resin with copper oxide and alumina using infra-red thermography . Besides, Moreira *et al.* (2014) studied the thermal conductivity dependence with temperature for polydimethilsiloxane nanocomposites with spherical particles of alumina and observed that this property increases with the particles addition (around 8,6%)and linearly decreases with the temperature. Another study made by Moreira *et al.* (2011) is the investigation of how much the thermal conductivity is effectively influenced by the alumina and copper oxide nanoparticles addition in a polyester resin, that showed that thermal conductivity increased 70% when the volumetric fraction was 10% of nanoparticles.

There are others studies that analysed the influence of the filler size and distribution in the composites thermal conductivity. Anhalt and Weidenfeller (2011) studied the influence of the filler amount and size in thermal conductivity of propilene and steel composites and observed that as higher is the filler amount, higher is the thermal conductivity. They also observed that the filler size don't have any influence in this property for the volumetric fraction studied (50%). Zhu *et al.* (2013) also analysed the filler size and amount effect in epoxy resin and aluminium nitrite composite thermal conductivity and observed similar results.

The purpose of this article is to develop a combined integral-transform finite-volumes solution to heat conduction problems in heterogeneous materials.

2. PROBLEM FORMULATION

Consider the problem of steady heat conduction with no heat generation in a heterogeneous media in a regular domain, given by the following PDE:

$$\frac{\partial}{\partial x}\left(k\frac{\partial T}{\partial x}\right)+\frac{\partial}{\partial y}\left(k\frac{\partial T}{\partial y}\right)=0 \tag{1}$$

for $x_a \le x \le x_b$ and $y_a \le y \le y_b$, with the following boundary conditions:

$$\left(\frac{\partial T}{\partial x}\right)_{x=x_a}=\left(\frac{\partial T}{\partial x}\right)_{x=x_b}=0, \tag{2}$$

$$(T)_{y=y_a}=a(x), \qquad (T)_{y=y_b}=b(x), \tag{3}$$

where $k=k(x,y)$.

The problem is normalized by introducing the following dimensionless quantities:

$$\Theta=\frac{T-T_{ref}}{\Delta T_{ref}}, \qquad k^*=\frac{k}{k_m}, \qquad \xi=2\,\frac{x-x_a}{x_b-x_a}-1, \qquad \eta=2\frac{y-y_a}{y_b-y_a}-1, \tag{4a}$$

$$\mathrm{K}=\frac{y_b-y_a}{x_b-x_a}, \tag{4b}$$

which leads to the non-dimensional form:

$$\mathrm{K}^2 \frac{\partial}{\partial \xi}\left(k^* \frac{\partial \Theta}{\partial \xi}\right) + \frac{\partial}{\partial \eta}\left(k^* \frac{\partial \Theta}{\partial \eta}\right) = 0, \tag{5}$$

$$\left(\frac{\partial \Theta}{\partial \xi}\right)_{\xi=\xi_a} = \left(\frac{\partial \Theta}{\partial \xi}\right)_{\xi=\xi_b} = 0, \tag{6}$$

$$(\Theta)_{\eta=\eta_a} = a(\xi), \tag{7}$$

$$(\Theta)_{\eta=\eta_b} = b(\xi), \tag{8}$$

2.1 Integral transform pair and eigenfunction basis

In order to transform the problem, the following Integral Transformation pair is used:

$$\overline{\Theta}_m(\eta) = \int_{\xi_a}^{\xi_b} \Theta(\xi,\eta)\, X_m(\xi)\, \mathrm{d}\xi, \tag{9a}$$

$$\Theta(\xi,\eta) = \sum_{m=0}^{\infty} \frac{\overline{\Theta}_m(\eta)\, X_m(\xi)}{N_m} \tag{9b}$$

where X_m are non-trivial solutions for the following eigenvalue problem:

$$X'' + \mu^2 X = 0, \tag{10}$$

which yields:

$$X_m = \cos\left(\mu_m\left(\xi - \xi_a\right)\right), \qquad \text{with} \qquad \mu_m = \frac{m\,\pi}{\xi_b - \xi_a} \tag{11}$$

for $m = 0, 1, 2, 3$. The norms N_m are given by:

$$N_m = \int_{\xi_a}^{\xi_b} X_m X_n \mathrm{d}\xi = \begin{cases} 0, & \text{for} \quad m \neq n \\ \frac{\xi_b - \xi_a}{2}, & \text{for} \quad m = n \neq 0 \\ \xi_b - \xi_a, & \text{for} \quad m = n = 0 \end{cases} \tag{12}$$

2.2 Hybrid Integral Transform Solution of Conduction Problem

The transformation of the problem is carried out by integrating equation (5) within $\eta_a \leq \eta \leq \eta_b$ and substituting the inverse formula (9b) to the non-transformable terms. For the η-diffusion terms this process yields:

$$\int_{\xi_a}^{\xi_b} \frac{\partial}{\partial \eta}\left(k^* \frac{\partial \Theta}{\partial \eta}\right) X_m \,\mathrm{d}\xi = \int_{\xi_a}^{\xi_b} \frac{\partial}{\partial \eta}\left(k^* \frac{\partial}{\partial \eta}\left(\sum_{n=0}^{\infty} \frac{\overline{\Theta}_n(\eta)\, X_n}{N_n}\right)\right) X_m \,\mathrm{d}\xi =$$
$$\frac{\mathrm{d}}{\mathrm{d}\eta} \sum_{n=0}^{\infty} \frac{1}{N_n} \int_{\xi_a}^{\xi_b} \left(\frac{\partial \overline{\Theta}_n(\eta)}{\partial \eta} k^*\, X_m\, X_n\right) \mathrm{d}\xi = \frac{\mathrm{d}}{\mathrm{d}\eta}\left(\sum_{n=0}^{\infty}\left(\frac{1}{N_n}\int_{\xi_a}^{\xi_b} k^*\, X_m\, X_n \,\mathrm{d}\xi\right)\frac{\mathrm{d}\overline{\Theta}_n}{\mathrm{d}\eta}\right) \tag{13}$$

while for the ξ-diffusion the transformation yields:

$$\mathrm{K}^2 \int_{\xi_a}^{\xi_b} \frac{\partial}{\partial \xi}\left(k \frac{\partial \Theta}{\partial \xi}\right) X_m \,\mathrm{d}\xi = \mathrm{K}^2 \left[\left(k^* \frac{\partial \Theta}{\partial \xi} X_m\right)_{\xi=\xi_a}^{\xi=\xi_b}\right] - \mathrm{K}^2 \int_{\xi_a}^{\xi_b} k^* \frac{\partial \Theta}{\partial \xi} X'_m \,\mathrm{d}\xi =$$
$$- \mathrm{K}^2 \int_{\xi_a}^{\xi_b} \frac{\partial}{\partial \xi}\left(\sum_{n=0}^{\infty} \frac{\overline{\Theta}_n(\eta) X_n}{N_n}\right) k^*\, X'_m \,\mathrm{d}\xi = -\sum_{n=0}^{\infty} \overline{\Theta}_n(\eta) \frac{\mathrm{K}^2}{N_n} \int_{\xi_a}^{\xi_b} k^*\, X'_n\, X'_m \,\mathrm{d}\xi \tag{14}$$

Finally, the transformation process yields the following infinite coupled ODE system:

$$\sum_{n=0}^{\infty}\left[\frac{\mathrm{d}}{\mathrm{d}\eta}\left(A_{m,n} \frac{\mathrm{d}\overline{\Theta}_n}{\mathrm{d}\eta}\right) - B_{m,n}\overline{\Theta}_n(y)\right] = 0 \tag{15}$$

valid for $m = 0, 1, 2, \ldots$, where the coefficients $A_{m,n}$ and $B_{m,n}$ are given, by the following expressions:

$$A_{m,n} = \frac{1}{N_n} \int_{\xi_a}^{\xi_b} k^*\, X_m\, X_n \,\mathrm{d}\xi \tag{16a}$$

$$B_{m,n} = \frac{\mathrm{K}^2}{N_n} \int_{\xi_a}^{\xi_b} k^*\, X'_n\, X'_m \,\mathrm{d}\xi \tag{16b}$$

The the boundary conditions for the coupled ODE system are obtained through the transformation of the original boundary conditions given by equations (7) and (8), which gives:

$$\left(\overline{\Theta}_n\right)_{\eta=\eta_a} = a_n(\xi), \tag{17a}$$

$$\left(\overline{\Theta}_n\right)_{\eta=\eta_b} = b_n(\xi), \tag{17b}$$

where the involved coefficients are given by:

$$\bar{a}_n = \int_{\xi_a}^{\xi_b} a(\xi)\, X_m \,\mathrm{d}\xi, \tag{18a}$$

$$\bar{b}_n = \int_{\xi_a}^{\xi_b} b(\xi)\, X_m \,\mathrm{d}\xi, \tag{18b}$$

While system (15) is in an infinite representation of the transformed problem it must be truncated before any solution can be applied. Truncating the infinite representation to a finite order gives the following system written in vector form:

$$\frac{\mathrm{d}}{\mathrm{d}\eta}\left(\boldsymbol{A}\,\frac{\mathrm{d}\overline{\boldsymbol{\Theta}}}{\mathrm{d}\eta}\right) - \boldsymbol{B}\,\overline{\boldsymbol{\Theta}} = \boldsymbol{0} \tag{19a}$$

$$\left(\overline{\boldsymbol{\Theta}}_n\right)_{\eta=\eta_a} = \bar{\boldsymbol{a}}_n(\xi), \tag{19b}$$

$$\left(\overline{\boldsymbol{\Theta}}_n\right)_{\eta=\eta_b} = \bar{\boldsymbol{b}}_n(\xi), \tag{19c}$$

2.2.1 Solution of transformed system using an ODE system solver

This coupled system can be solved directly using a commercially of publicly available dedicated ODE solver. While this is the traditional solution procedure amongst GITT users, when the resulting ODE system comprises a boundary value problem, the numerical solution using dedicated solvers can become prohibitively time-consuming. As an alternative, a simple second-order finite-volumes scheme is devised in the next section and solutions obtained with the two methodologies are compared in the results section.

2.2.2 Discretization of the transformed system

Rather than using the traditional GITT approach of solving the transformed system using a dedicated ODE system solver, an alternative solution based on a second-order finite volume method approach is employed. The discretization scheme is started by integrating equation (19a) within a finite volume $\eta_{p-1/2} \leq \eta \leq \eta_{p+1/2}$:

$$\left[\boldsymbol{A}\,\frac{\mathrm{d}\overline{\boldsymbol{\Theta}}}{\mathrm{d}\eta}\right]_{\eta_{p+1/2}}^{\eta_{p-1/2}} - \int_{\eta_{p-1/2}}^{\eta_{p+1/2}} \boldsymbol{B}\,\overline{\boldsymbol{\Theta}}\,\mathrm{d}\eta = \boldsymbol{0} \tag{20}$$

followed by the approximation of integrals with a second-order rule:

$$\left[\boldsymbol{A}\,\frac{\mathrm{d}\overline{\boldsymbol{\Theta}}}{\mathrm{d}\eta}\right]_{\eta_{p+1/2}}^{\eta_{p-1/2}} - \boldsymbol{B}^p\,\overline{\boldsymbol{\Theta}}_p\,\Delta\eta = \boldsymbol{0} \tag{21}$$

in which $\eta_p = \eta_a + p\,\Delta\eta/2$ and $\Delta\eta = (\eta_b - \eta_a)/p_{\max}$ is the uniform grid spacing. Then, the following second-order approximations are employed for the derivatives:

$$\left.\frac{\mathrm{d}\overline{\boldsymbol{\Theta}}}{\mathrm{d}\eta}\right|_{\eta_{p-1/2}} = \frac{\overline{\boldsymbol{\Theta}}^p - \overline{\boldsymbol{\Theta}}^{p-1}}{\Delta\eta}, \qquad \text{for} \quad p > 1, \tag{22a}$$

$$\left.\frac{\mathrm{d}\overline{\boldsymbol{\Theta}}}{\mathrm{d}\eta}\right|_{\eta_{p+1/2}} = \frac{\overline{\Theta}_n\big|_{p+1} - \overline{\boldsymbol{\Theta}}\big|_p}{\Delta\eta}, \qquad \text{for} \quad p < p_{\max}, \tag{22b}$$

$$\left.\frac{\mathrm{d}\overline{\boldsymbol{\Theta}}}{\mathrm{d}\eta}\right|_{\eta_{p-1/2}} = \frac{-8\,\bar{\boldsymbol{a}}_n + 9\,\overline{\boldsymbol{\Theta}}^p - \overline{\boldsymbol{\Theta}}_{p+1}}{3\,\Delta\eta}, \qquad \text{for} \quad p = 1, \tag{22c}$$

$$\left.\frac{\mathrm{d}\overline{\boldsymbol{\Theta}}}{\mathrm{d}\eta}\right|_{\eta_{p+1/2}} = \frac{\overline{\boldsymbol{\Theta}}^{p-1} - 9\,\overline{\boldsymbol{\Theta}}^p + 8\,\bar{\boldsymbol{b}}_n}{3\,\Delta\eta}, \qquad \text{for} \quad p = p_{\max}, \tag{22d}$$

such that a discretized system is obtained:

$$\boldsymbol{A}^{p+1/2}\frac{\overline{\boldsymbol{\Theta}}_{p+1}-\overline{\boldsymbol{\Theta}}^{p}}{\Delta\eta^2}-\boldsymbol{A}^{p-1/2}\frac{-8\,\bar{\boldsymbol{a}}+9\,\overline{\boldsymbol{\Theta}}^{p}-\overline{\boldsymbol{\Theta}}_{p+1}}{3\,\Delta\eta^2}-\boldsymbol{B}^{p}\,\overline{\boldsymbol{\Theta}}^{p}=\boldsymbol{0},\qquad \text{for}\quad p=1, \tag{23a}$$

$$\boldsymbol{A}^{p+1/2}\frac{\overline{\boldsymbol{\Theta}}_{p+1}-\overline{\boldsymbol{\Theta}}^{p}}{\Delta\eta^2}-\boldsymbol{A}^{p-1/2}\frac{\overline{\boldsymbol{\Theta}}^{p}-\overline{\boldsymbol{\Theta}}^{p-1}}{\Delta\eta^2}-\boldsymbol{B}^{p}\overline{\boldsymbol{\Theta}}^{p}=\boldsymbol{0},\qquad \text{for}\quad 1<p<p_{\max}, \tag{23b}$$

$$\boldsymbol{A}^{p+1/2}\frac{\overline{\boldsymbol{\Theta}}^{p-1}-9\,\overline{\boldsymbol{\Theta}}^{p}+8\bar{\boldsymbol{b}}}{3\,\Delta\eta^2}-\boldsymbol{A}^{p-1/2}\frac{\overline{\boldsymbol{\Theta}}^{p}-\overline{\boldsymbol{\Theta}}^{p-1}}{\Delta\eta^2}-\boldsymbol{B}^{p}\,\overline{\boldsymbol{\Theta}}^{p}=\boldsymbol{0},\qquad \text{for}\quad p=p_{\max}. \tag{23c}$$

This system can be rewritten in the following compact form

$$-\boldsymbol{D}^{p}\,\overline{\boldsymbol{\Theta}}_{p}+\boldsymbol{U}^{p}\,\overline{\boldsymbol{\Theta}}_{p+1}=-\bar{\boldsymbol{a}}^{+},\qquad \text{for}\quad p=1, \tag{24a}$$

$$\boldsymbol{L}^{p}\,\overline{\boldsymbol{\Theta}}_{p-1}-\boldsymbol{D}^{p}\,\overline{\boldsymbol{\Theta}}_{p}+\boldsymbol{U}^{p}\,\overline{\boldsymbol{\Theta}}_{p+1}=\boldsymbol{0},\qquad \text{for}\quad 1<p<p_{\max}, \tag{24b}$$

$$\boldsymbol{L}^{p}\,\overline{\boldsymbol{\Theta}}_{p-1}-\boldsymbol{D}^{p}\,\overline{\boldsymbol{\Theta}}_{p}=-\bar{\boldsymbol{b}}^{+},\qquad \text{for}\quad p=p_{\max}. \tag{24c}$$

in which:

$$\boldsymbol{D}^{p}=\boldsymbol{B}^{p}+\frac{3\,\boldsymbol{A}^{p-1/2}+\boldsymbol{A}^{p+1/2}}{\Delta\eta^2},\qquad \boldsymbol{U}^{p}=\frac{1}{3}\,\frac{\boldsymbol{A}^{p-1/2}}{\Delta\eta^2}+\frac{\boldsymbol{A}^{p+1/2}}{\Delta\eta^2},\qquad \text{for}\quad p=1, \tag{25a}$$

$$\boldsymbol{L}^{p}=\frac{\boldsymbol{A}^{p-1/2}}{\Delta\eta^2},\qquad \boldsymbol{D}^{p}=\boldsymbol{B}^{p}+\frac{\boldsymbol{A}^{p-1/2}+\boldsymbol{A}^{p+1/2}}{\Delta\eta^2},\qquad \boldsymbol{U}^{p}=\frac{\boldsymbol{A}^{p+1/2}}{\Delta\eta^2},\qquad \text{for}\quad 1<p<p_{\max}, \tag{25b}$$

$$\boldsymbol{L}^{p_{\max}}=\frac{\boldsymbol{A}^{p-1/2}}{\Delta\eta^2}+\frac{1}{3}\,\frac{\boldsymbol{A}^{p+1/2}}{\Delta\eta^2},\qquad \boldsymbol{D}^{p_{\max}}=\boldsymbol{B}^{p}+\frac{\boldsymbol{A}^{p-1/2}+3\,\boldsymbol{A}^{p+1/2}}{\Delta\eta^2},\qquad \text{for}\quad p=p_{\max}, \tag{25c}$$

$$\bar{\boldsymbol{a}}^{+}=\frac{8}{3}\,\frac{\boldsymbol{A}^{p-1/2}}{\Delta\eta^2}\,\bar{\boldsymbol{a}},\qquad \text{for}\quad p=1, \tag{25d}$$

$$\bar{\boldsymbol{b}}^{+}=\frac{8}{3}\,\frac{\boldsymbol{A}^{p+1/2}}{\Delta\eta^2}\,\bar{\boldsymbol{b}},\qquad \text{for}\quad p=p_{\max}, \tag{25e}$$

2.2.3 Tridiagonal block-matrix form

The previous system form can be written in a tridiagonal form when block matrices are considered:

$$\boldsymbol{M}\,\boldsymbol{y}=\boldsymbol{j}, \tag{26}$$

where

$$\boldsymbol{y}=\left(\overline{\boldsymbol{\Theta}}_{1},\overline{\boldsymbol{\Theta}}_{2},\ldots,\overline{\boldsymbol{\Theta}}_{p_{\max}}\right) \tag{27}$$

$$\boldsymbol{j}=\left(-\bar{\boldsymbol{a}}^{+},\boldsymbol{0},\boldsymbol{0},\ldots,\boldsymbol{0},-\bar{\boldsymbol{b}}^{+}\right) \tag{28}$$

and $\boldsymbol{M}$ is a tri-diagonal block matrix. For $p_{\max}=5$, it is given by:

$$\boldsymbol{M}=\left(\begin{array}{c|c|c|c|c} -\boldsymbol{D}^{1} & \boldsymbol{U}^{1} & \boldsymbol{0} & \boldsymbol{0} & \boldsymbol{0} \\ \hline \boldsymbol{L}^{2} & -\boldsymbol{D}^{2} & \boldsymbol{U}^{2} & \boldsymbol{0} & \boldsymbol{0} \\ \hline \boldsymbol{0} & \boldsymbol{L}^{3} & -\boldsymbol{D}^{3} & \boldsymbol{U}^{3} & \boldsymbol{0} \\ \hline \boldsymbol{0} & \boldsymbol{0} & \boldsymbol{L}^{4} & -\boldsymbol{D}^{4} & \boldsymbol{U}^{4} \\ \hline \boldsymbol{0} & \boldsymbol{0} & \boldsymbol{0} & \boldsymbol{L}^{5} & -\boldsymbol{D}^{5} \end{array}\right) \tag{29}$$

Finally, the solution of system (26) can be directly obtained by a linear system solution routine. In *Mathematica* this is accomplished by the function **LinearSolve**.

3. TEST CASES

In order to analyze the temperature field convergence, two shapes and orientations for the cross section of the filler were considered: a square filler and a circular filler, as shown in Fig. 1, where k^{*} varies as

$$k^{*}(\xi,\eta)=\left\{\begin{array}{l} k^{*}_{\max},-(\frac{\xi_b-\xi_a}{2}-\frac{\delta^{*}}{2})<\xi<(\frac{\xi_b-\xi_a}{2}-\frac{\delta^{*}}{2})\quad and\quad -(\frac{\eta_b-\eta_a}{2}-\frac{\delta^{*}}{2})<\eta<(\frac{\eta_b-\eta_a}{2}-\frac{\delta^{*}}{2}) \\ 1,\eta<-(\frac{\eta_b-\eta_a}{2}-\frac{\delta^{*}}{2})\quad,\quad \eta>(\frac{\eta_b-\eta_a}{2}-\frac{\delta^{*}}{2})\quad,\quad \xi<-(\frac{\xi_b-\xi_a}{2}-\frac{\delta^{*}}{2})\quad,\quad \xi>(\frac{\xi_b-\xi_a}{2}-\frac{\delta^{*}}{2}) \end{array}\right. \tag{30}$$

for the square disperse phase and

$$k^{*}(\xi,\eta)=\left\{\begin{array}{l} k^{*}_{\max},-\sqrt{\frac{\delta^{*2}}{4}-\xi^{2}}<\eta<\sqrt{\frac{\delta^{*2}}{4}-\xi^{2}} \\ 1,\eta<-\sqrt{\frac{\delta^{*2}}{4}-\xi^{2}}\quad and\quad \eta>\sqrt{\frac{\delta^{*2}}{4}-\xi^{2}} \end{array}\right. \tag{31}$$

for the circular disperse phase , in which $k^{*}_{\max}$ is the normalized filler thermal conductivity and δ^{*} is defined in figure 1.

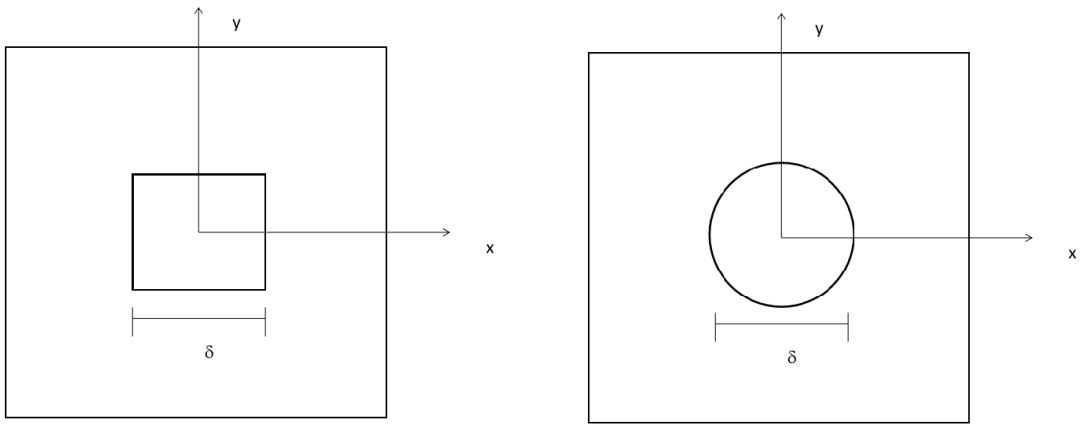

Figura 1: **Shape and orientation of considered fillers.**

4. RESULTS

4.1 Convergence analysis of temperature field

The convergence analysis of the temperature field is based on examining the temperature at select points, as displayed in Table 1.

Tabela 1: **Points observed in convergence analysis.**

Θ_1	$\Theta(0, \delta^*/2)$
Θ_2	$\Theta(0, \delta^*/4)$
Θ_3	$\Theta(0, \delta^*/2 + (\eta_b - \delta^*/2)/2)$
Θ_4	$\Theta(0, \eta_b)$
Θ_5	$\Theta(\delta^*/4, \delta^*/2)$
Θ_6	$\Theta(\delta^*/4, \delta^*/4)$
Θ_7	$\Theta(\delta^*/2 + (\xi_b - \delta^*/2)/2, \delta^*/4)$
Θ_8	$\Theta(\xi_b, \delta^*/4)$

Table 2 displays the convergence results for dispersed phase consisting of a square region, while table 3 portrays the convergence results for a circular region. The results are calculated for a dimensionless inclusion size $\delta^* = 1/2$, thermal conductivity ratio $k^*_{\max} = 10$, prescribed temperatures $a_n = 0$ and $b_n = 1$, ξ_a= η_a= -1/2 and ξ_b= η_b=1/2. As can be seen from these results using $n_{\max} = 40$ and $p_{\max} = 50$ yield two-converged digits, which is a satisfactory result in many applications. Also, we can observe that the results for point Θ_4 are close to 1 which is the prescribed temperature at the top surface.

Tabela 2: **Temperature convergence for selected points using a square disperse phase with $\delta^* = 1/2$ and $k^*_{\max} = 10$.**

$n_{\max}$	$p_{\max}$	Θ_1	Θ_2	Θ_3	Θ_4	Θ_5	Θ_6	Θ_7	Θ_8
20	50	0.5552	0.5294	0.7810	0.9945	0.5368	0.5313	0.5725	0.5853
20	100	0.5622	0.5292	0.7847	0.9973	0.5363	0.5310	0.5722	0.5851
20	200	0.5591	0.5294	0.7829	0.9986	0.5365	0.5312	0.5721	0.5850
20	400	0.5576	0.5295	0.7820	0.9993	0.5366	0.5313	0.5721	0.5849
20	800	0.5568	0.5296	0.7816	0.9996	0.5366	0.5314	0.5720	0.5849
40	50	0.5547	0.5292	0.7809	0.9945	0.5363	0.5312	0.5735	0.5864
40	100	0.5614	0.5290	0.7846	0.9973	0.5358	0.5308	0.5733	0.5864
40	200	0.5583	0.5292	0.7829	0.9986	0.5360	0.5311	0.5732	0.5863
40	400	0.5567	0.5293	0.7820	0.9993	0.5361	0.5312	0.5732	0.5862
40	800	0.5559	0.5294	0.7815	0.9996	0.5361	0.5312	0.5731	0.5861
60	50	0.5547	0.5292	0.7809	0.9945	0.5361	0.5311	0.5740	0.5866
60	100	0.5615	0.5289	0.7846	0.9973	0.5356	0.5307	0.5738	0.5866
60	200	0.5584	0.5292	0.7829	0.9986	0.5358	0.5310	0.5737	0.5864
60	400	0.5569	0.5293	0.7820	0.9993	0.5359	0.5311	0.5737	0.5863
60	800	0.5561	0.5293	0.7815	0.9996	0.5360	0.5311	0.5737	0.5863
80	50	0.5547	0.5292	0.7809	0.9945	0.5360	0.5311	0.5742	0.5868
80	100	0.5614	0.5289	0.7846	0.9973	0.5355	0.5307	0.5741	0.5868
80	200	0.5583	0.5291	0.7829	0.9986	0.5357	0.5309	0.5740	0.5866
80	400	0.5567	0.5292	0.7820	0.9993	0.5358	0.5310	0.5739	0.5866
80	800	0.5559	0.5293	0.7815	0.9996	0.5359	0.5311	0.5739	0.5865
100	50	0.5546	0.5291	0.7809	0.9945	0.5365	0.5310	0.5743	0.586
100	100	0.5614	0.5289	0.7846	0.9973	0.5354	0.5307	0.5744	0.5869
100	200	0.5583	0.5291	0.7829	0.9986	0.5357	0.5309	0.5741	0.5867
100	400	0.5568	0.5292	0.7820	0.9993	0.5358	0.5310	0.5740	0.5866
100	800	0.5560	0.5293	0.7815	0.9996	0.5358	0.5311	0.5740	0.5866
120	50	0.5546	0.5291	0.7809	0.9945	0.5360	0.5310	0.5743	0.5869
120	100	0.5614	0.5289	0.7846	0.9973	0.5354	0.5307	0.5742	0.5869
120	200	0.5583	0.5291	0.7829	0.9986	0.5367	0.5309	0.5741	0.5868
120	400	0.5567	0.5292	0.7820	0.9993	0.5357	0.5310	0.5741	0.5867
120	800	0.5559	0.5293	0.7815	0.9996	0.5358	0.5311	0.5740	0.5867

Tabela 3: **Temperature convergence in selected points for $\delta^* = 1/2$ and $k^*_{\max} = 10$ with a circular disperse phase.**

$n_{\max}$	$p_{\max}$	Θ_1	Θ_2	Θ_3	Θ_4	Θ_5	Θ_6	Θ_7	Θ_8
20	50	0.5552	0.5276	0.7915	0.9948	0.5408	0.5276	0.5880	0.5995
20	100	0.5622	0.5274	0.7937	0.9974	0.5408	0.5274	0.5881	0.5995
20	200	0.5565	0.5275	0.7929	0.9987	0.5408	0.5275	0.5881	0.5995
20	400	0.5565	0.5275	0.7926	0.9993	0.5408	0.5275	0.5881	0.5995
20	800	0.5556	0.5275	0.7924	0.9996	0.5408	0.5275	0.5881	0.5995
40	50	0.5539	0.5275	0.7918	0.9949	0.5458	0.5273	0.5893	0.5995
40	100	0.5615	0.5273	0.7942	0.9974	0.5458	0.5271	0.5894	0.5996
40	200	0.5584	0.5274	0.7936	0.9987	0.5459	0.5272	0.5894	0.5996
40	400	0.5568	0.5274	0.7933	0.9993	0.5459	0.5272	0.5894	0.5996
40	800	0.5558	0.5274	0.7932	0.9996	0.5345	0.5272	0.5894	0.5996
60	50	0.5545	0.5274	0.7919	0.9949	0.5471	0.5273	0.5897	0.5996
60	100	0.5616	0.5271	0.7944	0.9974	0.5473	0.5271	0.5899	0.5998
60	200	0.5583	0.5272	0.7938	0.9987	0.5474	0.5271	0.5899	0.5998
60	400	0.5566	0.5273	0.7936	0.9993	0.5474	0.5271	0.5899	0.5998
60	800	0.5558	0.5273	0.7935	0.9996	0.5474	0.5271	0.5899	0.5998
80	50	0.5545	0.5273	0.7920	0.9949	0.5360	0.5311	0.5742	0.5868
80	100	0.5616	0.5271	0.7945	0.9974	0.5473	0.5270	0.5900	0.5999
80	200	0.5583	0.5272	0.7940	0.9987	0.5473	0.5271	0.5900	0.5999
80	400	0.5565	0.5272	0.7937	0.9993	0.5473	0.5271	0.5900	0.5999
80	800	0.5557	0.5272	0.7936	0.9996	0.5473	0.5271	0.5900	0.5999
100	50	0.5543	0.5273	0.7920	0.9949	0.5476	0.5272	0.5899	0.5998
100	100	0.5616	0.5270	0.7945	0.9974	0.5477	0.5270	0.5902	0.6000
100	200	0.5583	0.5271	0.7940	0.9987	0.5478	0.5270	0.5902	0.6001
100	400	0.5566	0.5272	0.7938	0.9993	0.5478	0.5271	0.5902	0.6001
100	800	0.5556	0.5272	0.7937	0.9996	0.5478	0.5271	0.5902	0.6001
120	50	0.5544	0.5273	0.7920	0.9949	0.5477	0.5272	0.5900	0.5999
120	100	0.5616	0.5270	0.7460	0.9974	0.5481	0.5270	0.5902	0.6001
120	200	0.5583	0.5271	0.7941	0.9987	0.5481	0.5270	0.5902	0.6001
120	400	0.5565	0.5272	0.7939	0.9993	0.5481	0.5270	0.5902	0.6001

4.2 Temperature field

Fig. 2 and Fig. 3 show the temperature field found for the square and circular cross sections when $n_{\max} = 40$ and $p_{\max} = 50$. As can be seen from these figures, the temperature field shows that the temperature gradient is lower inside

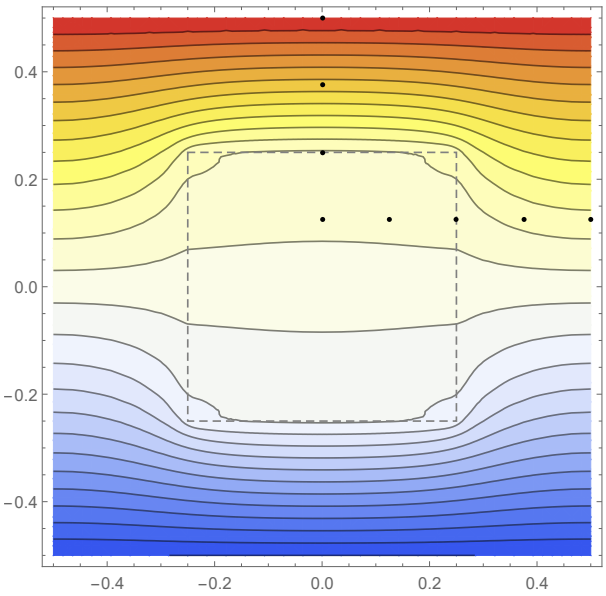

Figura 2: **Temperature field (square shape).**

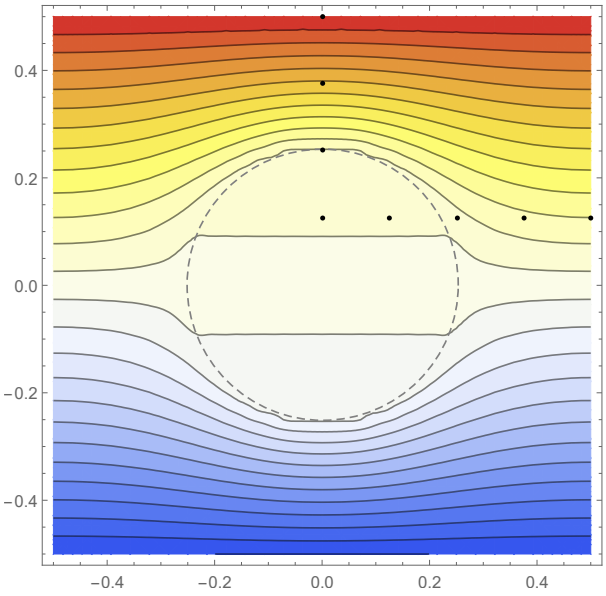

Figura 3: **Temperature field (circular shape).**

the disperse phase area than outside, which is expected since it has higher thermal conductivity.

5. SUMMARY AND CONCLUSIONS

This paper presented a hybrid methodology for solving the problem of heat conduction in heterogeneous media. A two-dimensional steady linear heat conduction problem was considered. The solution of the problem was carried out by means of the Generalized Integral Transform Technique, which transforms the original PDE system into an infinite boundary-value ODE system. This system was truncated and solved by employing a second-order uniform-grid finite volumes scheme. The results show that 40 terms in the series and 50 divisions grid divisions are sufficient for yielding data with about 1% of error (second digit convergence).

6. REFERENCES

Agrawal, A. and Satapathy, A., 2015. "Mathematical model for evaluating effective thermal conductivity of polymer composites with hybrid fillers". *International Journal of Thermal Sciences*, Vol. 89, pp. 203–209.

Anhalt, M. and Weidenfeller, B., 2011. "Influence of filler content, particle size and temperature on thermal diffusivity of polypropylene-iron silicon composites". *Journal of Applied Polymer Science*, Vol. 119.

Lee, G.W., Parka, M., Kima, J., Lee, J.I. and Yoon, H.G., 2006. "Enhanced thermal conductivity of polymer composites filled with hybrid filler". *Science Direct*, Vol. Part A 37.

Moreira, D.C., Benevides, R.O., Junior, N.R.B., Sphaier, L.A. and Nunes, L.C.S., 2014. "Temperature dependent thermal conductivity of silicone-al2o3 nanocomposites". *Composites: Part A*.

Moreira, D., Sphaier, L., Reis, J. and Nunes, L., 2011. "Experimental investigation of heat conduction in polyester-al2o3 and polyester-cuo nanocomposites". *Experimental Thermal and Fluid Science*, Vol. 35.

Moreira, D.C., Telles, M.C.O., Sphaier, L.A. and Nunes, L.C.S., 2015. "Infrared thermography for estimating the thermal conductivity augmentation of polymeric nanocomposites". *High Temperatures. High Pressures (Print)*, Vol. 44, pp. 3–23.

Shi, Z., Radwan, M., Kirihara, S., Miyamoto, Y. and Jin, Z., 2009. "Enhanced thermal conductivity of polymer composites filled with three-dimensional brushlike aln nanowhiskers". *Applied Physics Letters*, Vol. 95, No. 224104, pp. 1–3.

Zhao, J., Jiang, J.W., Wei, N., Zhang, Y. and Rabczuk, T., 2013. "Thermal conductivity dependence on chain length in amorphous polymers". *Journal Of Applied Physics*, Vol. 113, p. 184304.

Zhu, B.L., Wang, J., Ma, J., Wu, J., Yung, K.C. and Xie, C.S., 2013. "Preparation and properties of aluminum nitride-filled epoxy composites: Effect of filler characteristics and composite processing conditions". *Journal of Applied Polymer Science*.

7. AUTHOR RESPONSABILITY

The authors are the only responsible for the printed material included in this paper.